Journal of
Ceramic Science
and Technology

J. Ceram. Sci. Tech., 02 [01] 55-60 (2011)
DOI: 10.4416/JCST2010-00020
available online at: http://www.ceramic-science.com

Sintering and Mechanical Properties of $AlMgB_{14}$ Composite Materials

M. Herrmann*[1], R. Bodkin[2], N. J. Coville[2], I. Sigalas[3] and M. Thiele[1]

[1]Fraunhofer Institute of Ceramic Technologies and Systems, Dresden, Germany
[2]DST/NRF Centre of Excellence in Strong Materials and Molecular Sciences Institute, School of Chemistry, University of the Witwatersrand, Johannesburg, South Africa.
[3]DST/NRF Centre of Excellence in Strong Materials at the School of Chemical and Metallurgical Engineering, University of the Witwatersrand, Johannesburg, South Africa.
received May 26, 2010; received in revised form July 21, 2010; accepted September 24, 2010

Abstract

Different $AlMgB_{14}$ composite materials were prepared from pre-reacted $AlMgB_{14}$ and starting elemental powders by hot pressing. Only slightly different densification behaviours were found for the two types of starting materials. Full densification without decomposition was achieved only with a hot pressing pressure of 75 MPa. Different additives were tested to improve densification. The influence of the additives on the densification was found to be minor. A strong increase in hardness was observed for materials with Si, TiC, WC, TiB_2 additions. The carbides react with the $AlMgB_{14}$ during sintering, forming TiB_2 and WB_2 or their solid solutions.

Keywords: Boride, sintering, microstructure, $AlMgB_{14}$

I. Introduction

Modern industry operates increasingly under extreme circumstances, demanding materials that exhibit high wear resistance under different conditions. Therefore the search for new super-hard and wear-resistant materials is a main thrust in the field of materials development. To date, super-hard materials have been based on diamond and cubic boron nitride. However, a disadvantage is that high pressure (several GPa) is necessary for the production of these materials.

Hardness approaching the microhardness of cBN was found for several boron-rich compounds: (B_4C [1], B_6O (45 GPa measured on single crystals) [2-4] $B_{22}O$ (60 GPa $HV_{0.08}$ [5]) or doped ß-rombohedral boron with microhardness up to 45 GPa [6]. The boron-rich compounds are all based on the B_{12}. icosahedral units. Another compound having a similar structure is $AlMgB_{14}$ [7].

The hardness of pure nanocrystalline $AlMgB_{14}$ has been reported to range between 32 – 35 GPa [8]. The microhardness of the crystals has been measured and values of 25.8 GPa recorded [9]. Computational results suggest that the high hardness of $AlMgB_{14}$ is primarily related to the intrinsic hardness of the B_{12} icosahedral units and is less related to the linkage of the B_{12} icosahedra by Al and Mg [10]. An analysis of the electron density distribution reveals that the magnesium and aluminium atoms are predominantly ionically bonded to the icosahedra. The calculations also show that the most stable composition is not the stoichiometric one and in the stable structure only about ¾ of the position of the cation sites are occupied [11]. This has also been confirmed by investigations of the crystal structures [7, 12]. In summary, a consideration of all the physical data indicates that the exact composition of $AlMgB_{14}$ is not completely known. Therefore, in this paper $AlMgB_{14}$ will be used as the synonym for $Al_{1-x}Mg_{1-x}B_{14}$ ($x < 0{,}25$).

Pure $MgAlB_{14}$ has been reported to have a Vickers hardness (HV_1) value of 27.9 GPa [12]. It has been observed that $AlMgB_{14}$ composites containing TiB_2 and Si have hardness values exceeding that of $AlMgB_{14}$ [8] (35 – 46 GPa), but unfortunately the applied load used in the measurement was not given. No increase in the hardness value on addition of up to 50 wt% of TiB_2 was found. Ahmed *et al.* [13, 14] have observed an increase of the hardness and wear resistance with the addition of up to 80 wt% TiB_2. The reason for this hardening is still not clear. The fracture toughness of the materials was determined as 3.0 – 3.5 $MPam^{1/2}$ for the pure material [13, 15] with a slight increase on the addition of TiB_2 [13]. The addition of TiC resulted in a reduction of the hardness value [13].

The synthesis of $AlMgB_{14}$ has been performed based on high-energy milling of the elemental powders in hardened stainless steel vials for 12 to 20 hours [8, 15]. The most common impurity phase observed by Cook *et al.* [8] was the spinel phase $MgAl_2O_4$ and Fe contaminants. The lowest impurity level observed was between 2 and 10 vol% These powders were hot pressed at 1400 °C to 1500 °C and 100 – 140 MPa under a He atmosphere [8] or densified by spark plasma sintering (SPS) at 1400 to 1500 °C at 125 and 63 MPa pressure respectively [15].

Recently the phase composition in the system Al-Mg-B was investigated. The data showed that $AlMgB_{14}$ is in equilibrium with liquid Al at temperatures higher than 1200 °C [16]. Therefore the possibility exists that an excess

* Corresponding author: mathias.herrmann@ikts.fraunhofer.de

of Al could be used as a sintering additive for liquid phase sintering.

From the above overview, it is clear that materials based on $AlMgB_{14}$ could be suitable materials for wear applications. However, the existing data regarding the synthesis, composition, structure and properties of these materials does not provide a basis for their reproducible preparation. The aim of this paper was to prepare and investigate the properties of $AlMgB_{14}$ as a pure material as well as to determine its interaction with different suitable reinforcing components.

II. Experimental

Two sets of $AlMgB_{14}$ materials were prepared:

- The first set of materials was produced starting with the elemental powders. It was surmised that the chemical reaction could accelerate the densification. These materials were labelled E.
- The second set of materials was prepared by densification of a pre-reacted $AlMgB_{14}$ powder. These samples are labelled PR.

All materials and the pre-reacted powder were prepared from powders of Al (50 µm grain size, 99.9 % pure, Saarchem), Mg (70 µm grain size, 99.9 %, Saarchem) and B (2 - 5 µm grain size, 99.5 % pure, Johnson Matthey). The reinforcing components used were TiB_2 (1 – 2 µm grain size, HC STARCK) and WC (1 – 2 µm grain size, HC STARCK). Table 1 contains the composition data for the $AlMgB_{14}$ materials prepared from the elemental powders (Set 1). All samples (Table 1) were prepared from the elemental powders by wet milling in methanol for 2 hours in an Ar atmosphere in a planetary ball mill with WC milling media (Pulverisette 5, Fritsch). Milling in Ar helps reduce the oxidation of the $AlMgB_{14}$, but oxidation cannot be completely avoided. Therefore the $AlMgB_{14}$ powders always contain some oxygen owing to the surface oxide layers of the powders. This resulted in the formation of $MgAl_2O_4$. In the case of our experiments the $MgAl_2O_4$ formed after hot pressing was 8 wt% (corresponding to 4 vol%). This is consistent with results reported by Lewis *et al.* [17]. The use of methanol as milling media also reduces the amount of oxygen in the sample by removing the B_2O_3 present on the surface of B or formed as a result of oxidation during milling.

Table 1: Mass percentages for $AlMgB_{14}$ materials.

Name	Composition, wt%		
	Al	**Mg**	**B**
E	13.3	12.0	74.7
ES	19.2	13.6	67.2
ES3Al	21.5	13.2	65.3
ES5Al	23.0	13.0	64.0
ES10Al	26.5	12.4	61.1
Pre-reacted powder	19.1	13.6	67.2

The effect of the formation of $MgAl_2O_4$ on the ratio of the elements in the material has to be taken into account. The material with the corrected composition is labelled ES or in the case of the pre-reacted powder, PRS. Additionally, materials were prepared by addition of an excess of 3, 5 or 10 wt% aluminium to the reactants (Table 1).

Once the milling cycle was completed the powder was removed from the milling vessel and the solvent was removed in a rotary evaporator. The powder was sieved through a 38-µm sieve.

The pre-reacted powder was prepared by reaction of the stoichiometric amount of the elements at 1400 °C for 1 h in an Ar atmosphere.

XRD analysis of the powders showed that they contained only $AlMgB_{14}$ and some $MgAl_2O_4$. This powder was additionally milled for 2 h. The mean grain size after two hours was 7 µm. Increasing the milling time resulted in the formation of smaller grain sizes, but also a higher content of WC impurity, the WC coming from the milling process. SEM analysis of the pre-reacted powder showed that the size of the crystallites was in the range of 1 – 2 µm and that the grains are agglomerated (Fig. 1).

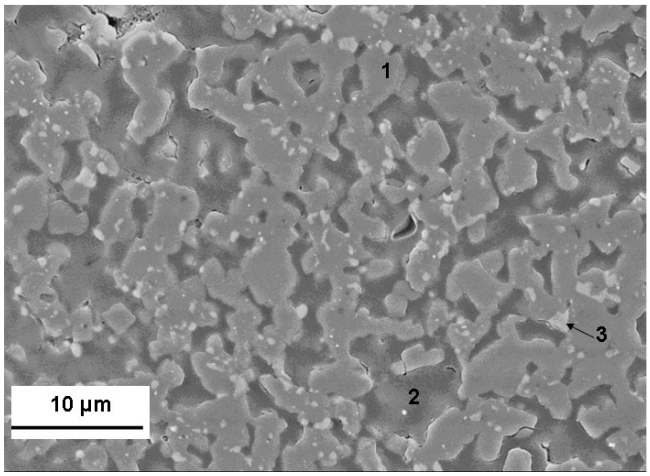

Fig. 1: SEM Micrograph of the polished cross-section of the pre-reacted powder before milling (the hard powder compact was infiltrated by mounting resin and polished; 1- $AlMgB_{14}$, 2- resin, 3- $MgAl_2O_4$).

The compositions of the composites investigated are listed in Table 2. The amount of the additional components was chosen such that they form MB_2 phases with the same volume content (20 vol%), e.g. 25.6 wt% TiC 30 wt% TiB_2. Therefore the PRS 30TiB_2 and PRS 25.8TiC samples are directly comparable. The added carbides are not stable and react with $AlMgB_{14}$, forming less boron-rich borides with lower hardness. To compensate for this decomposition in some of the materials, additional B was added, e.g. the amount of boron in PRS25.8TiC+B was calculated on the basis of the following reaction:

$TiC + 6B \rightarrow TiB_2 + B_4C$.

The mixtures were additionally milled for 2 h to mix the pre-reacted powder with the additives. Also the material with no additives was milled for 2 h to allow direct comparison with the above data. The resulting mean grain size of all the samples was 2 µm. The procedure for the powder preparation was the same as that used for the synthesis of the elemental powders.

Table 2: Compositions for the composites.

Composite	Pre-reacted $AlMgB_{14}$ powder	Additive	added B	Phase composition after sintering
	Wt%	Wt%	Wt%	
PRS	100.00			$AlMgB_{14}$, $MgAl_2O_4$ *, W_2B_4*
PRS 5Si	95.00	5.00	0.00	$AlMgB_{14}$, $MgAl_2O_4$*, W_2B_4*
PRS 30TiB_2	70.00	30.00	0.00	$AlMgB_{14}$, (Ti,W)B_2 $MgAl_2O_4$*
PRS 25.8TiC	74.16	25.84	0.00	$AlMgB_{14}$, (Ti,W)B_2 $MgAl_2O_4$*
PRS 25.8TiC+B	57.90	20.20	21.90	$AlMgB_{14}$, (Ti,W)B_2, $MgAl_2O_4$*
PRS 46(WC TiB_2)	53.85	46.00	0.00	$AlMgB_{14}$, (Ti,W)B_2, W_2B_4, $MgAl_2O_4$*
PRS46(WC TiB_2)+B	46.20	39.60	14.20	$AlMgB_{14}$, (Ti,W)B_2, W_2B_4, $MgAl_2O_4$*
PRS+30WC	70.00	30.00		$AlMgB_{14}$, W_2B_4, $MgAl_2O_4$*

* present in small amounts

The samples were hot pressed (HP20; Thermal Technology) in a hBN-lined graphite die in an argon atmosphere at temperatures up to 1700 °C and pressures of 20 – 70 MPa for 1 hour. The various phases were measured by X-ray diffraction (XRD 7, Seifert FPM; step size 0.02°, 2θ range 12-110°). Mounted samples were polished with a 9-µm diamond grit, a 6-µm diamond grit, a 3-µm diamond grit and finally with a 1-µm diamond grit, all at 300 rpm.

Polished samples were analysed with Vickers hardness testers. The hardness was determined at a load of 98 N. Fracture toughness was evaluated based on indentation fracture toughness measurements as in [14, 15] using the Anstis formula [18]. The elastic constant was taken from [19, 24]. The ratio of c/a in the measurements was between 2.5 and 3. The authors realize that the fracture toughness measurement method is not the standard one and gives values which can be systematically shifted in comparison to the values determined with the standard method [25], but it allows at least comparison of the materials with the data observed in the literature based on the same method [12 – 15]. Bending bars for the accurate SEVNB method were not available. Therefore further fracture toughness measurements are necessary.

III. Results and Discussions

The synthesis of $AlMgB_{14}$ was achieved from elemental powders of Al, Mg and B that were pressed into green compacts and then hot-pressed in the temperature range 1200 – 1700 °C (soak time 1 hour) at 20 MPa. Additionally some experiments were conducted at higher pressure. $AlMgB_{14}$ was formed at temperatures above 1200 °C. At 1700 °C evaporation of Mg was observed, which resulted in the formation of detectable amounts of AlB_{12}. The decomposition of $AlMgB_{14}$ into γ-AlB_{12} at temperatures above 1600 °C is consistent with literature reports stating that $AlMgB_{14}$ decomposes into γ-AlB_{12} at temperatures higher than 1550 °C [8, 17]. At an applied pressure of 20 MPa none of the materials could be densified, even at 1700 °C (Fig. 2). The higher density of the pre-reacted powder (PR) is primarily caused by the higher starting density and not caused by better densification behaviour.

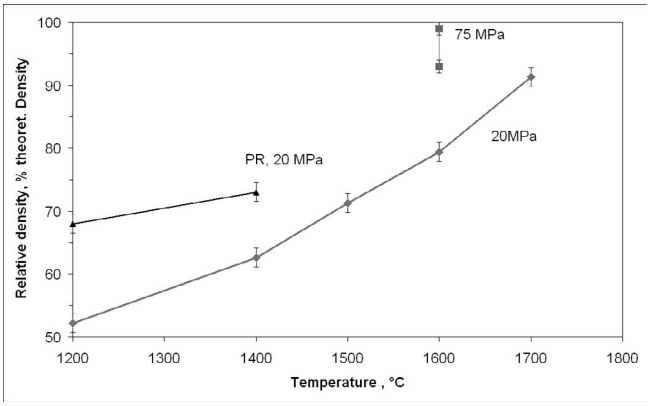

Fig. 2: Dependence of the densification of the material E on the temperature at 20 MPa and 75 MPa pressure; additionally the data for the PR samples at 1200 and 1400 °C are given.

From the preliminary experiments, the optimum density for limited decomposition was found to be achieved at 1600 °C. Hence, subsequent samples were prepared at 1600 °C and 75 MPa.

$AlMgB_{14}$ + Al: In a second series of experiments the influence of an excess of Al on the densification of $AlMgB_{14}$ was tested. The results (Fig. 3) revealed that an excess of aluminium has no positive influence on the densification behaviour. The densification process with excess Al is independent of the use of the pre-reacted powder or the elemental powder. The densification of the elemental powder is slightly better than that observed for the pre-reacted powder.

The microstructures of the materials ES3Al and PRS3Al are shown in Fig. 4. The micrographs showed that the materials produced by densification of the elemental powders

have a pronounced texture. This was the case also for the other prepared samples (E and ES). A variation of the pressure application did not help. The inhomogeneous structure thus obtained was the reason that the composites were produced using the pre-reacted powder route in this work. It is possible that intensive high-energy milling, which results in at least partial formation of the borides during the milling, can prevent such texture in the materials.

The density of the composites (Table 3) was found to be in the range of 95 – 99 % of the theoretical densities. The observed hardness $HV_{10} = 24.0 \pm 1.9$ GPa of the PRS material is in agreement with the HV_1 data observed for $MgAlB_{14}$ (26 – 28 GPa) [12–15].

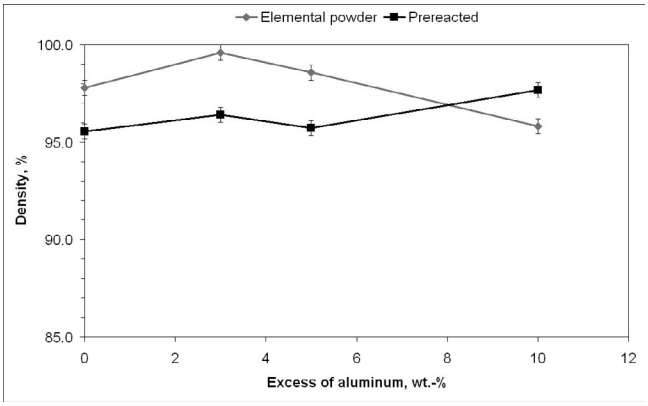

Fig. 3: Density of the materials prepared from the starting elemental powders and the pre-reacted powders at 1600 °C and 75 MPa as a function of the excess of aluminium in the composition (materials ES, ES3Al,ES5Al, ES10Al and PRS...PRS10 Al).

$AlMgB_{14}$ + WC: The small amounts of WC introduced either by milling or by actual WC addition react with the $AlMgB_{14}$ to form W_2B_4 (not W_2B_5 [20]). In PRS samples the formation of W_2B_4 was confirmed by EDX and XRD analysis. Additionally the carbon from the WC additive could be expected to form some boron carbide. However, the presence of the B_4C could not be confirmed either by XRD measurements or from SEM micrographs.

Table 3: Density, porosity, Vickers hardness and fracture toughness of the composites.

Composite	Density (gcm^{-3})	HV_{10} (GPa)	K_{IC} ($MPam^{1/2}$)
PRS	3.05±0.01	24.0±1.9	4.7±1.0
PRS30 TiB_2	3.41±0.01	29.5±1.7	3.8±0.6
PRS5 Si	3.02±0.01	31.2±1.5	4.3±1.1
PRS25.8TiC	3.43±0.01	32.1±2.7	3.5±0.8
PRS25.8TiC + B	3.19±0.01	30.9±2.3	3.8±0.8
PRS30WC	3.62±0.01	17.1±1.2	5.5±0.8
PRS46(TiB_2 WC)	4.27±0.01	29.1±1.6	4.5±0.8
PRS46(WC TiB_2)+B	3.93±0.01	33.8±1.4	5.0±0.8

$AlMgB_{14}$ + TiB_2: The data reveal TiB_2 is in equilibrium with $AlMgB_{14}$. Therefore in this material no change in the composition takes place. The WC introduced by milling precipitates on the surface of the TiB_2 grains as W_2B_4 (Fig. 5). Both compounds – TiB_2 and W_2B_4 – have similar structures and epitaxial growth of the formed W_2B_4 on the TiB_2 can be expected. Also some mutual solubility of both compositions exists. In the TiB_2-W_2B_4 system the solubility range decreases to around 8 – 10 mol% WB_2 in TiB_2 at 1500 °C [21]. The growth of WB_2 platelets can also be initiated by heterogeneous nucleation close to the grain boundaries of the $(Ti,W)B_2$ grains [22, 23]. Such platelet-like growth of the W_2B_4 was also partially determined in the PRS+30WC sample.

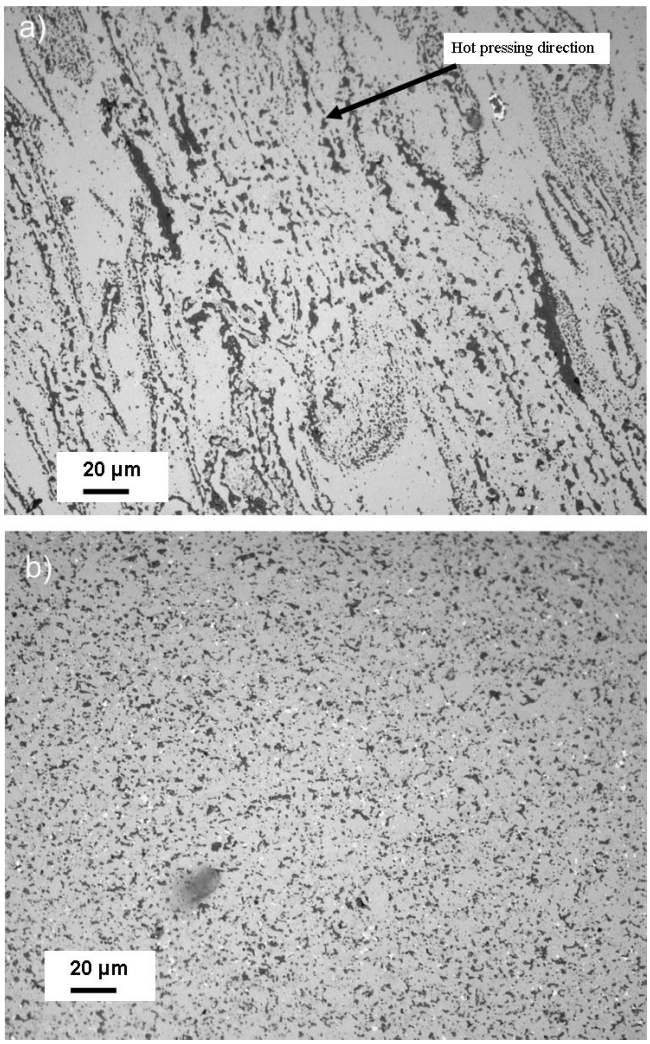

Fig. 4: Light microscope image of Material ES3AL (a) and PRS3Al densified at 1600 °C and 75 MPa (b).

$AlMgB_{14}$ + TiC: TiC is not in the equilibrium with $MgAlB_{14}$ and it can react with $MgAlB_{14}$ to form TiB_2 in the following reaction:

$$2TiC + AlMgB_{14} \rightarrow 2TiB_2 + (Al,Mg)B_2 + 2B_4C$$

The formation of TiB_2 was observed with both XRD and SEM analysis. The presence of the $(Al,Mg)B_2$ phase was not clearly identified by XRD and neither was B_4C. The main peaks in the XRD pattern of the solid solution $(Al,Mg)B_2$ overlap with the other phases and would have only a low intensity. Therefore small amounts of the $(Al,Mg)B_2$ phase will not be detectable.

Additionally the carbon can partially react with the oxides to form CO. The peaks in the XRD pattern of the $MgAl_2O_4$ are slightly reduced, but do not disappear completely. Therefore the role of the carbon as an additive to $AlMgB_{14}$ is not completely clear. Sigl has mentioned the possibility of reduction of oxide scales in B_4C-TiB_2 composites by using carbon [23]. While the reduction of B_2O_3 is possible as a consequence of the reaction with carbon, the reduction of Al_2O_3 is not possible under the applied conditions (thermodynamic calculations using the FACTSAGE program). Carbon can enhance only the evaporation of Al_2O_3 owing to increased Al_2O gas formation.

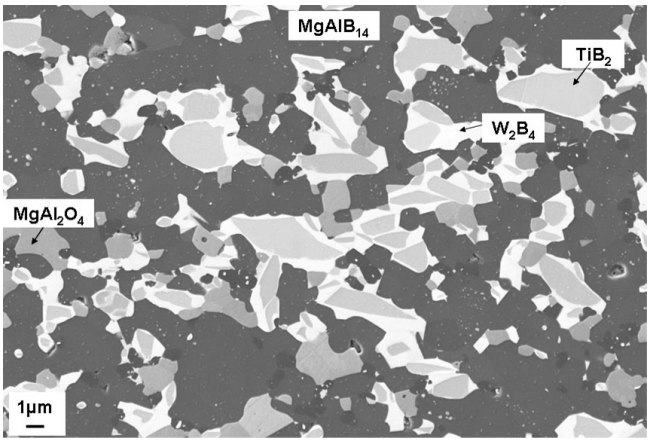

Fig. 5: SEM micrograph of the material PRS30TiB_2.

The addition of amorphous B will reduce the decomposition of $AlMgB_{14}$ caused by TiC:

$$TiC + 6B \rightarrow TiB_2 + B_4C$$

This addition does not result in visible changes in the phase composition and the microstructure of the material. TiB_2- and WB_2-rich solid solutions form in the material with the combined additives WC and TiB_2.

$AlMgB_{14}$ + Si: Addition of 5 wt% Si to $AlMgB_{14}$ yielded an increase in hardness. EDX measurements on the $AlMgB_{14}$ grains in the material PRS5Si reveal an incorporation of approximately 1 at% Si in the $AlMgB_{14}$. Another Si containing compound could not be detected with XRD analysis.

The hardness and the fracture toughness values of all the materials prepared in this study are given in Table 3. The data reveal that the addition of TiB_2, TiC, or TiB_2/WC increases the hardness in comparison to the PRS materials. The properties of the AlB_{14}/TiB_2 composites are in agreement with the previous data[8, 12-14]. The addition of TiB_2 or TiC results in nearly the same values independently of any reaction taking place during sintering. The compensation of the B, which would be consumed by reaction with the carbide, does not result in significant changes in the mechanical properties.

The material with only WC addition shows the lowest hardness. This is probably caused by the slightly higher porosity (5 %) and the lower intrinsic hardness of W_2B_4 that is formed in the reaction (26 – 27 GPa in comparison with 34 GPa for TiB_2 GPa [24]). Similar high hardness values (32 GPa) and fracture toughness values (4 – 5 $MPam^{1/2}$) were determined for the B_4C-TiB_2-WB_2 composite[23]. The increase in the fracture toughness of this material was attributed to the internal stresses generated by the different thermal expansion coefficients and enhanced crack deflection of the W_2B_4 platelets. A similar toughening mechanism can take place in the case of $MgAlB_{14}$-based composites. The differences in the thermal expansion coefficients are not as pronounced in the $AlMgB_{14}$-materials and therefore also the toughening mechanism is less pronounced. Additionally the (W,Ti)B_2 inclusions are under compression and not under tension as in the B_4C composite materials. This can explain the nearly constant fracture toughness values measured.

The reason for the pronounced change of the hardness on addition of small amounts of silicon is not completely clear. Beside the incorporation of Si into $AlMgB_{14}$ other mechanisms could be responsible for the behaviour. A similar effect of Si additions has been found for HIPed B_4C-TiB_2-W_2B_4 [23]. This effect needs further investigation using TEM.

IV. Conclusions

Different $AlMgB_{14}$ composite materials were prepared and their fracture toughness and hardness were measured. The densification was strongly dependent on the applied pressure. This has been found for other materials containing a high amount of boron. This makes the commercial use of these materials less attractive. The attempt to accelerate densification by the addition of some extra Al, which forms a liquid phase under sintering conditions, was not successful. The final density was nearly independent of the excess of aluminium added to the material.

The "pure" $AlMgB_{14}$ materials contained a small amount of $MgAl_2O_4$ and a small amount of W_2B_4. The $MgAl_2O_4$ formation is caused by the oxidation of surface layers of the starting powders. The WB_2 is formed by reaction with the milling media, WC.

The 98-% dense, pure $AlMgB_{14}$ has a HV_{10} hardness of 24 GPa. The addition of 30 wt% WC, which transforms during densification into W_2B_4, reduces the hardness of the material, but the addition of TiC increases the hardness. Therefore it can be expected that the hardness of the $AlMgB_{14}$ materials increases slightly if the WC content (approx. 5 – 8 wt%) can be reduced by more sophisticated processing procedures.

The composites made by addition of TiC, TiB_2 or TiB_2/WC to $AlMgB_{14}$ show a significant increase in hardness in comparison with the pure $AlMgB_{14}$. This could be caused by the change in the grain boundary chemistry and structure. Further, the intrinsic high hardness of TiB_2 and solid solutions of W_2B_4 with TiB_2 could also enhance the hardness.

It was found by EDX measurements that some Si incorporates into the lattice of $AlMgB_{14}$. This can be one reason for the increased hardness of the Si-doped materials.

Further detailed microstructural analysis of this promising group of wear-resistant materials is necessary to understand their mechanical properties.

References

1 Werheit, H., Leithe-Jasper, A., Tanaka, T., Rotter, H.W., Schwetz, K.A.: Some properties of single-crystal boron carbide, *J. Solid State Chem.*, **177**, 575-579, (2004).

2 He, D., Zhao, Y., Daemen, L., Qian, J., Shen, T.D., Zerda, T.W.: Boron suboxide: As hard as cubic boron nitride, *Appl. Phys. Lett.*, **81**, 643-645, (2002).

3 Nieto-Sanz, D., Loubeyre, P., Crichton, W., Mezouar, M.: X-ray study of the synthesis of boron oxides at high pressure: Phase diagram and equation of state, *Phys. Rev. B*, **70**, 214108, (2004).

4 Itoh, H., Maekawa, I., Iwahara, H.: High pressure sintering of B_6O powder and properties of the sintered compact, *J. Soc. Mat. Sci., Japan*, **47**, 1000-1005, (1998).

5 Badzian, A.R.: Applied Physics Letters, **53**, 2495-2497, (1988).

6 Hebache, M.: The Search for Superhard Materials: Doped boron, EPL, 87, 16001, (2009).

7 Higashi, I., Ito, T.: Refinement of the structure of magnesium aluminum boride ($MgAlB_{14}$), *J. Less Common Met.,* **92**, 239-46, (1983).

8 Cook, B.A., Harringa, J.L., Lewis, T.L., Russell, A.M.: A new class of ultra-hard materials based on $AlMgB_{14}$, *Scripta Mater.*, **42**, 597-602, (2000).

9 Okada, S., Shishido, T., Mori, T., Iizumi, K., Kudou, K., Nakajima, K.: Crystal growth of $MgAlB_{14}$-type compounds using metal salts and some properties, *J. Alloy Compd.*, **458**, 297-301, (2008).

10 Lowther, J.E.: Possible ultra-hard materials based upon boron icosahedra, *Physica B, Condensed Matter*, **322**, 173-178, (2002).

11 Kölpin, H., Music, D., Henkelman, G., Schneider, J.M.: Phase stability and elastic properties of $XMgB_{14}$ studied by *ab initio* calculations (X=Al,Ge,Si,C,Mg,Sc,Ti,V,Zr,Nb,Ta,Hf), *Physical Review B*, **78**, 054122, (2008).

12 Kevorkijan, V., Skapin, S.D., Jelen, M., Krnel, K., Meden, A.: Cost-effective synthesis of $AlMgB_{14}$-xTiB_2, *J. Eur. Cer. Soc.*, **27**, 493-497, (2007).

13 Ahmeda, A., Bahadura, S., Cook, B.A., Peters, J.: Mechanical properties and scratch test studies of new ultra-hard $AlMgB_{14}$ modified by TiB_2, *Tribol. Int.*, **39,** 129-137, (2006).

14 Ahmeda, A., Bahadur, S., Russell, A.M., Cook, B.A.: Belt abrasion resistance and cutting tool studies on ultra-hard boride materials, *Tribol. Int.*, **42**, 706-713, (2009).

15 Roberts, D.J., Zhao, J., Munir, Z.A.: Mechanism of reactive sintering of $MgAlB_{14}$ by pulse electric current, *Int. J. Refract. Met. H.*, **27**, 556-563, (2009).

16 Bodkin, R., Herrmann, M., Coville, N.J., Sigalas, I.: A study of the Al-MgB ternary phase diagram, *Int. J. Mat. Res.* (formerly Z. Metallkd.), **100**, 105-109, (2009).

17 Lewis, T.L., Cook, B.A., Harringa, J.L., Russell, A.M.: Al_2MgO_4, Fe_3O_4 and FeB impurities in $AlMgB_{14}$, *Mat. Sci. and Eng. A*, **351**, 117, (2003).

18 Anstis, G.R., Chantikul, P., Lawn, B.R., Marshall, D.B.: A critical evaluation of indentation techniques for measuring fracture toughness: I. Direct crack measurements, *J. Amer. Ceram. Soc.*, **64**, 533-8, (1981).

19 Yongbin, L., Harmon, B.N.: First principles calculation of elastic properties of $AlMgB_{14}$, *J. Alloy. Compd.*, **338**, 242-247, (2002).

20 Frotscher, M., Klein, W., Bauer, J., Fang, C.M., Halet, J.F., Senyshyn, A., Baehtz, C., Albert, B.: A Reinvestigation of the Mo/B and W/B System, *Z. Anorg. Allg. Chem.*, **633**, 2626, (2007).

21 Telle, R., Fendler, E., Petzow, G.: The quasi-binary systems CrB_2-TiB_2, CrB_2-WB_2, TiB_2-WB_2, *J. Hard. Mat.*, **3**, 211-224, (1992)

22 Mitra, I., Telle, R.: Phase formation during anneal of supersaturated TiB_2-CrB_2-WB_2 solid solutions, *J. Solid State Chem.*, **133**, 25, (1997).

23 Telle, R., Sigl, L.S., Takagi, K.: Boride-based Hard Materials, R. Riedel, Handbook of Ceramic Hard Materials, Wiley-VCH, 802-933, (2000).

24 Riedel, R.: Handbook of Ceramic Hard Materials, Wiley-VCH, 968, (2000).

25 Quinn, G., Bradt, R.: On the Vickers Indentation Fracture Toughness Test, *J. Am. Ceram. Soc.*, **90**, 673, (2007)